



Thermal degradation mechanisms of PEDOT:PSS

E. Vitoratos^{a,*}, S. Sakkopoulos^a, E. Dalas^b, N. Paliatsas^a, D. Karageorgopoulos^a, F. Petraki^c, S. Kennou^c, S.A. Choulis^d

^a Department of Physics, University of Patras, 265 00 Patras, Greece

^b Department of Chemistry, University of Patras, 265 00 Patras, Greece

^c Department of Chemical Engineering, University of Patras, 265 00 Patras, Greece

^d Department of Mechanical Engineering and Materials Science and Engineering, Cyprus University of Technology, 3603 Limassol, Cyprus

ARTICLE INFO

Article history:

Received 4 July 2008

Received in revised form 5 October 2008

Accepted 7 October 2008

Available online 21 October 2008

PACS:

72.80.-r

73.61.Ph

82.35.Cd

Keywords:

Conducting polymers

Conductivity degradation mechanisms

Thermal stability

PEDOT/PSS

Organic light emitting diodes

Organic solar cells

ABSTRACT

The thermal stability of thin (50 nm) PEDOT:PSS films, was investigated by dc conductivity measurements, X-ray and UV photoelectron spectroscopies as a function of heating temperature and heating time. The mechanism of electrical conductivity as a function of temperature is consistent with a hopping type carrier transport. The electrical conductivity decreased, as a function of time, in agreement with a granular metal type structure, in which aging is due to the shrinking of the PEDOT conductive grains. XPS and UPS spectra indicate that conformational changes of the PEDOT:PSS film are responsible for this behaviour and a model for these modifications is proposed.

© 2008 Elsevier B.V. All rights reserved.

1. Introduction

Organic semiconductors are of increasing interest as new materials for optoelectronic devices. This class of semiconductors is processed from solution, offering a huge potential for low fabrication costs and flexibility. Polymer emitting diodes (PLEDs), photodiodes and solar cells are the optoelectronic applications under intense study [1]. One of the fundamental requirements for reliable operation of all organic optoelectronic devices is a stable anode interface. Indium tin oxide (ITO) has been the preferred anode for all organic optoelectronic devices due to its optical

transparency and high conductivity [1–3]. However, the work function of ITO is quite low (even after special ITO treatment procedures such as plasma or oxygen treatment) [4]. The most common way to improve hole injection/collection is to incorporate a hole transporting layer (buffer layer) on top of the ITO surface [4,5]. The most common buffer layer is the poly(ethylenedioxythiophene):polystyrene sulphonate (PEDOT:PSS) [5].

Poly(3,4-ethylenedioxythiophene) (PEDOT), a π -conjugated polymer, combines high electrical conductivity with excellent optical transparency [6]. The problem with its low solubility is solved by the use of the water soluble polyelectrolyte poly(styrene sulfonic acid) PSS as a charge balancing dopant. PEDOT mixed with PSS forms an easily processible colloidal solution in water. For organic

* Corresponding author. Tel.: +30 2610 997487; fax: +30 2610 997428.
E-mail address: vitorato@physics.upatras.gr (E. Vitoratos).

optoelectronic applications PEDOT:PSS is an essential part of the bottom electrode providing a high selective carrier contact. The stability of PEDOT:PSS layer is of high importance and determines the lifetime performance of organic optoelectronic devices. Despite the common use of PEDOT:PSS the correlation between the electrical conductivity and the morphology and especially the irreversible structural changes occurring during thermal degradation are not fully understood [7,8]. The purpose of this investigation is to study the thermal aging of the electrical conductivity of PEDOT:PSS thin films and correlate this with the morphological, composition and electronic structure changes occurring during the thermal degradation.

2. Methods

2.1. Materials

All measurements performed on 50 nm PEDOT:PSS films coated on pristine plastic substrates (PET). An aqueous dispersion of PEDOT:PSS (CLEVIOS PH 500, H.C. Starck) was used, where the ratio PEDOT-to-PSS was 1:2.5 by weight.

2.2. Conductivity measurements

Temperature dependence d.c. conductivity measurements $\sigma = \sigma(T)$ performed using a four-probe method. For the temperature dependent studies a He filled cryostat was used [9]. Samples from the same PEDOT:PSS film were thermally treated at 120 °C in a thermostated oven under environmental conditions for different times. The 0 h time includes only the annealing step during the preparation process 20 min. The conductivity versus temperature was then measured after the heat treatment at every time. These successive measurements give a set of $\sigma = \sigma(T)$ curves and the whole procedure is repeated until saturation in conductivity is observed.

2.3. X-ray photoelectron and ultra-violet photoelectron spectroscopies

X-ray photoelectron spectroscopy (XPS) was used to investigate the variation in the chemical structures of the sample surface of the PEDOT:PSS films before and after the thermal degradation, while the variation of the PEDOT:PSS valence band was investigated by ultra-violet photoelectron spectroscopy (UPS). The photoelectron spectroscopy measurements were carried out in a commercial ultra-high vacuum (UHV) system which consists of a fast entry specimen assembly, a preparation and an analysis chamber. The analysis chamber is equipped with a hemispherical electron analyzer (SPECS LH-10), a twin anode X-ray gun and a discharge lamp for X-ray and ultra-violet photoelectron spectroscopy (XPS and UPS) measurements. The base pressure was 5×10^{-10} mbar. The XPS measurements were carried out with a non-monochromatic Mg K α line at 1253.6 eV and a constant analyzer pass energy of 36 eV, while for UPS the He I (21.22 eV) radiation was used. The spectrometer was calibrated by the Au4f $_{7/2}$ core

level (84.00 ± 0.05 eV) for a clean Au foil. The XPS resolution, measured by the full width at half maximum (FWHM) of the Au4f $_{7/2}$, was 1.10 eV for a constant pass energy of 36 eV. The analyzer resolution for the UPS measurements is determined from the width of the Au Fermi edge and is found 0.16 eV. A negative bias of 12.30 V was applied to the sample during UPS measurements in order to separate sample and analyzer high binding energy cut-offs and estimate the absolute work function from the UV photoemission spectra.

3. Results and discussion

In Fig. 1 the d.c. conductivity σ as a function of temperature T is shown for PEDOT:PSS exposed to thermal treatment times ranging from 0 to 55 h at 120 °C. The mechanism of carrier (hole polarons) transport in PEDOT:PSS is determined by its morphology. Conductive PEDOT oligomers consisted of 5–15 repeat units are electrostatically attached to twisted long insulating PSS chains, which form grains 20–70 nm in diameter, whose surfaces are rich in PSS [10,11]. So, in PEDOT:PSS, with its granular structure of conductive PEDOT-rich grains enclosed in insulating PSS-rich shells, the electrical conductivity is not determined only from the hole polarons transport into the PEDOT segments, but also by their hopping between segments and grains.

Despite different interpretations of the temperature dependence of the experimentally obtained conductivities, typically $\sigma = \sigma(T)$ is given by

$$\sigma(T) = \sigma_0 \exp \left[- \left(\frac{T_0}{T} \right)^\alpha \right] \quad (1)$$

which generally describes a hopping transport, where T_0 is a measure of the potential barrier height, as carriers get thermally activated hopping among localized states at different energies [12–14]. On the other hand σ_0 is related to the intrinsic conductivity of the grains, their size contribution, mean volume occupied by the conducting grains in the material, etc. [15].

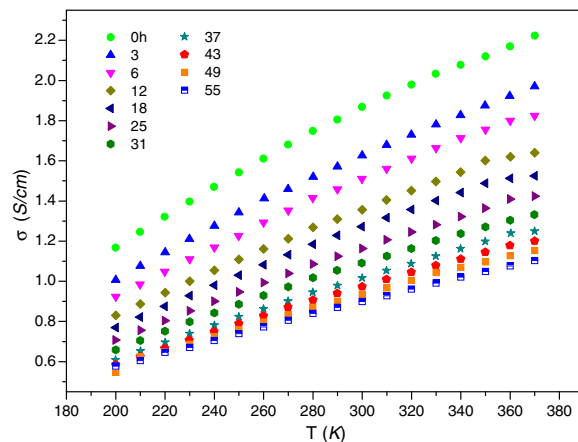


Fig. 1. Thermal degradation of the d.c. electrical conductivity of a 50 nm thick PEDOT:PSS film heated at 120 °C under environmental conditions for times between 0 and 55 h.

In a material consisting of conductive grains embedded into an insulating matrix, thermal degradation can be considered as a corrosion – a process which is reducing the size of the grains and consequently enhancing their distance, or equivalently increasing the potential barrier for polaron transport between them. In this case the conductivity can be described by the following equation

$$\ln \sigma = \sigma_1 \exp[-(t/\tau)^{1/2}] \quad (2)$$

in which t is the time of the thermal treatment and τ is a parameter characteristic of the aging rate. The higher the τ value, the slower the rate of degradation [16].

In the variable-range hopping (VRH) model of transport the exponent α in Eq. (1) does not depend only on the number of the hopping process dimensions D , but also on the exponent μ of the density of states $g(E) \propto (E-E_F)^\mu$ near the Fermi energy level E_F , according to the formula $\alpha = \mu + 1/(\mu + D + 1)$ [17].

In disordered systems, in which a self-assembled network of conductive polymer, PEDOT in our case, spreads in a matrix of insulating PSS, the carrier eigenstates display spatial fluctuations described by a multifractal analysis, in which the electrical conductivity follows Eq. (1) with the exponent α decreasing systematically from 1 to 0.25 with increasing the volume fraction of the conductive component [18,19]. The exponent $\alpha = 1$ indicates a nearest-neighbor hopping (nn-H) between PEDOT particles [12]. On the other hand, hopping conductivity in granular disordered systems follows Eq. (1) with the exponent α ranging from 0.25 to 1 depending on the distribution of grain sizes. The decrease of the particle size results in the reduction of the exponent α from values about unity to 0.5 or 0.25 [20]. An exponent $\alpha = 0.25$ is consistent to a three-dimensional VRH, though an exponent $\alpha = 1/2$ can be attributed to many cases. For example, the existence of an energy gap caused by Coulomb interactions between the carriers results in a $\alpha = 1/2$. However, the non-zero density of states at the Fermi level reveals that such an energy gap does not exist in PEDOT:PSS [12]. Another explanation for the $\alpha = 1/2$ value is in the framework of the charging-energy limited tunnelling (CELT) model, where carriers tunnel between small conductive grains separated by insulating material [21,22]. From the above it is apparent that the exponent α can reveal valuable information about the conduction mechanism in PEDOT:PSS.

In Fig. 2 the exponent α of Eq. (1) is shown for increasing heat treatment time at 120 °C. For the fresh samples ($t = 0$ h) $\alpha \approx 1$ decreasing with thermal aging to the value $\alpha \approx 0.5$ at the end of it, after 55 h of heat treatment. Taken into account the morphology of PEDOT:PSS, this means that for the first stages of the heat treatment, the nearest-neighbor hopping prevails, though later the charging-energy limited tunnelling between adjacent conductive grains determines the conduction. For $\alpha \sim 1$, Eq. (1) takes the well known Arrhenius formula, from which the mean of the potential barrier height can be estimated to $E \sim 0.022 \pm 0.001$ eV for the fresh samples.

XPS and UPS were used to investigate the composition and electronic structure changes due to the thermal aging process. In Fig 3 the XPS spectra S 2p for PEDOT:PSS sam-

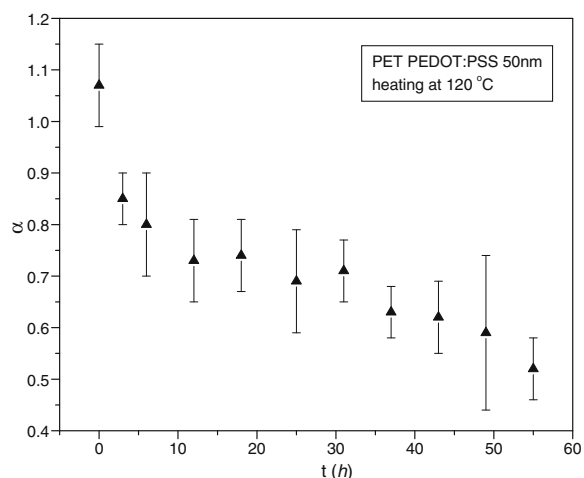


Fig. 2. The exponent α of Eq. (1) vs. thermal treatment time for the same PEDOT:PSS sample, as in Fig. 1.

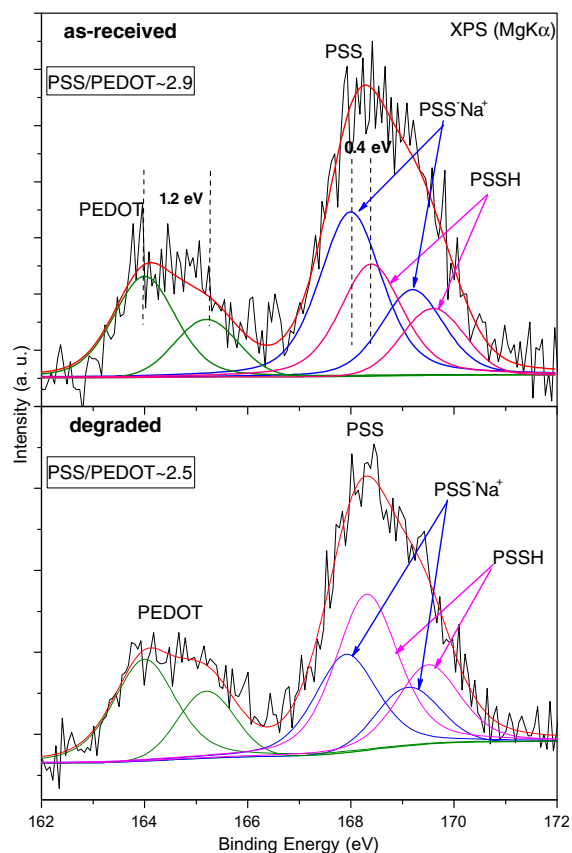


Fig. 3. S(2p) spectra from (a) a fresh PEDOT:PSS sample and (b) from the same sample after heat treatment at 120 °C under environmental conditions for 55 min.

ples (a) fresh and (b) after heat treatment at 120 °C for 55 h are shown. In both cases the S 2p spectrum appears in two components. The component at lower binding energies is attributed to the contribution of PEDOT and in particular,

to sulphur atoms linked to carbon in the chemical structure of PEDOT and the peak at higher binding energies corresponds to the sulphur atoms in the PSS polymer. The spectra were fitted with mixed Gaussian–Lorentzian peaks after Shirley background subtraction. The PEDOT component is fitted in all cases with a single spin-orbit doublet at 164.0 ± 0.1 eV and 165.2 ± 0.1 eV binding energy and a 2p_{3/2} to 2p_{1/2} ratio of 2:1, the splitting of 1.2 eV being that expected for S 2p. The contribution of PSS to the S 2p peak is due to the doping ions PSS[−]H⁺ (spin-orbit doublet at 168.4 eV and 169.6 eV binding energy) and to the PSS[−]Na⁺ salt [23,24] (spin-orbit doublet at 168.0 eV and 169.2 eV binding energy). Na⁺ residues originate from Na₂S₂O₈ oxidizing agent used during the polymerization of PEDOT [25]. The original ratio of PSS-Na to the PSS-H in the PSS layer is found equal to 1.5 and it drops to 0.6 after the heat treatment. From them it can be seen that there is a decrease of the PSS-Na bond in the PSS chains due to thermal aging. The PEDOT-to-PSS ratio in the surface region can be calculated from the total area under the S2p core level spectra and it was found 1:2.9 for the PEDOT:PSS before thermal degradation. After thermal degradation up to 55 h at 120 °C this ratio becomes 1:2.4. As has also reported before for the fresh PEDOT:PSS the spectra indicate that there is phase segregation with an excess of PSS [25]. During this work we show that after 55 h at 120 °C the excess of PSS is slightly reduced.

In order to estimate the thickness d of the outermost PSS layer, we consider PSS and PEDOT as two separated polymers growing in the form of a “layer over layer” structure ending in a pure PSS layer and compare the intensities from the contribution to the S2p peak of each polymer. The thickness is given by the expression

$$d = \lambda \ln[(I_{\text{PSS}}/I_{\text{PSS}}^0)/(I_{\text{PEDOT}}/I_{\text{PEDOT}}^0) + 1] \quad (3)$$

where $\lambda = 2.7 \pm 0.3$ nm, is the electron inelastic mean free path, and I_x, I_x^0 are the measured and expected signal intensities from species X , respectively [23]. The above equation yields an outermost PSS layer thickness of 3.6 nm for the PEDOT:PSS before thermal degradation and 3.4 nm after thermal aging at 120 °C for 55 h, verifying that there is a thinning of the PSS layer on the surface.

From UPS spectra of the same PEDOT:PSS sample before and after the heat treatment at 120 °C, it can be seen that the density of the electronic states near the Fermi level slightly increases, although the work function of the surface decreases from 4.7 eV for the fresh sample to 3.7 eV at the end of the heat treatment. These can be attributed to the removal of the insulating PSS from the surface, which leaves an area enriched in PEDOT, from which is easier to remove carriers and as a p-doped conjugated polymer has occupied valence band states near the Fermi level [26].

From Fig. 3 it can also be seen that the peaks corresponding to the PSSH bond diminish with aging. This indicates that there is enough energy for the breaking of the electrostatic bonding between PSS and PEDOT, which gradually leads to the reeling off the PSS chains and on the other hand to the formation of PEDOT-rich clusters between the PSS chains [13,23].

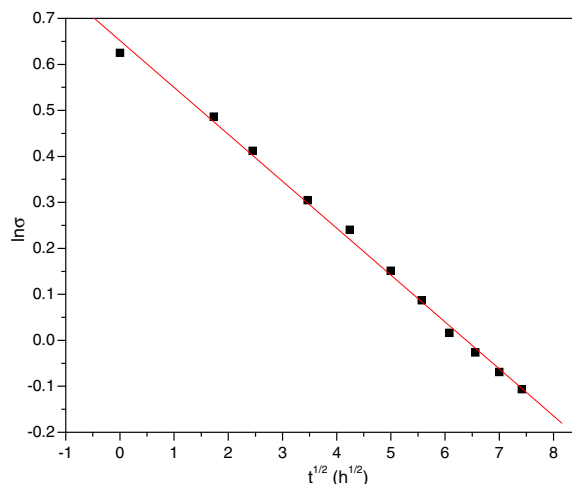


Fig. 4. $\ln \sigma = f(t^{1/2})$ experimental data at 300 K for heating temperature 120 °C.

From Fig. 4 it is shown that for heating temperature 120 °C the experimental data follow very well Eq. (2). Moreover, from the fitting of the experimental data, the parameter τ takes the value 96 h and from Eq. (2) it can be calculated that the time of heating, for the conductivity of the sample to become half of its original value, is 46.1 h, in excellent agreement with the experiment, from which this time is 46.3 h. This is consistent with a granular structure of PEDOT:PSS and an electrical conductivity degradation, in which the main contribution comes from the progressive increase of the potential barriers between the conductive grains with heat treatment.

The above experimental results can be explained by the following model of conformational changes during the thermal aging. At the first stage of heating, the PSS chains are perplexed, as it is shown in Fig. 5 and the agitation of the Cl[−] ions (their existence is verified by EDX spectrograms) attached weakly to the hole polarons on the PEDOT

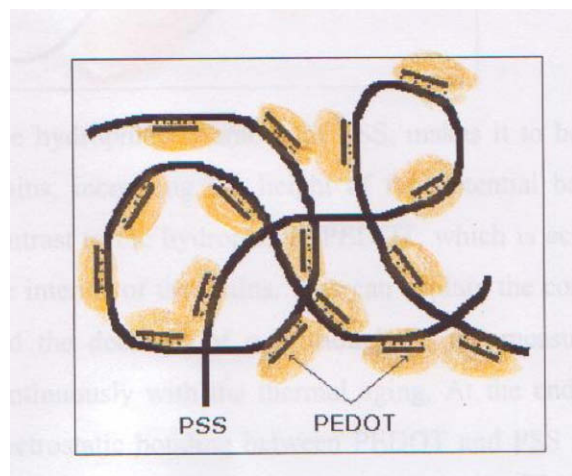


Fig. 5. Perplexed PSS chains at the first stage of heating.

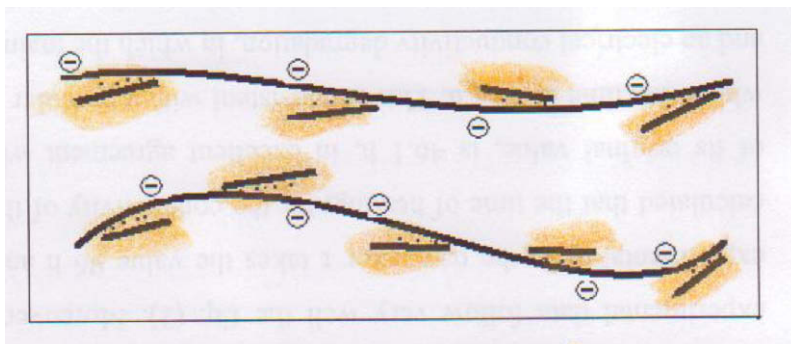


Fig. 6. The ionic bonds between PEDOT and the PSS chains start to break.

oligomers, makes them to wander further away from the polaron vicinity, increasing the mobility of the latter. This makes the grains more conductive as it is revealed from the decrease of the exponent α and the increase of σ_0 .

At a second stage of the heat treatment, shown in Fig. 6, the ionic bonds between the PEDOT oligomers and the PSS chains start to break.

The remaining negative charges on the PSS chains repulse each other resulting in an improvement of their alignment. In this stage the conductive PEDOT oligomers concentrate between the aligned PSS chains forming grains of enhanced conductivity, as it is shown in Fig. 7.

The hydrophilic character of PSS, makes it to be concentrated at the surface of the grains, increasing the height of the potential barriers, as this stage progresses, in contrast to the hydrophobic PEDOT, which is accumulated in increasing numbers in the interior of the grains. This can explain the continuous decrease of the exponent α and the decrease of σ_0 , although T_0 , the measure of the barriers height increases continuously with the thermal aging. At the end of the heat treatment, most of the electrostatic bonding between PEDOT and PSS is removed, as it is revealed by the XPS spectrograms.

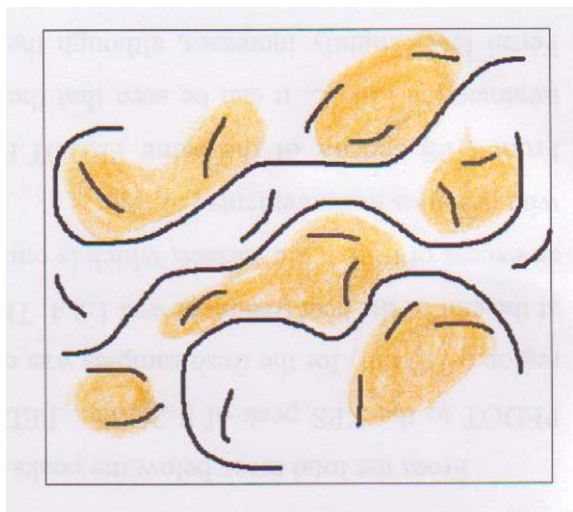


Fig. 7. PEDOT oligomers start to form conducting grains.

From Fig. 4 it is shown that for heating temperature 120 °C the experimental data follow very well Eq. (2). Moreover, from the fitting of the experimental data, the parameter τ takes the value 96 h and from Eq. (2) it can be calculated that the time of heating, for the conductivity of the sample to become half of its original value, is 46.1 h, in excellent agreement with the experiment, from which this time is 46.3 h. This is consistent with a granular structure of PEDOT:PSS and an electrical conductivity degradation, in which the main contribution comes from the progressive increase of the potential barriers between the conductive grains with heat treatment.

From the total areas below the peaks representing the contribution of PSS and PEDOT to the XPS peak of S2p, the PEDOT-to-PSS molar ratio in the surface region (~ 10 nm) for the fresh samples was estimated to 1:2.9, though for the samples at the end of the heat treatment was 1:2.4. This indicates that in fresh samples there is an excess of PSS at the surface, which is removed by the heat treatment, in agreement with previous measurements [23–25].

From UPS spectra of the same PEDOT:PSS sample before and after the heat treatment at 120 °C, it can be seen that the density of the electronic states near the Fermi level slightly increases, although the work function of the surface decreases from 4.7 eV for the fresh sample to 3.7 eV at the end of the heat treatment. These can be most likely attributed to the removal of the insulating PSS from the surface, which leaves an area enriched in PEDOT, from which is easier to remove carriers and as a p-doped conjugated polymer has occupied valence band states near the Fermi level [26]. As has already been reported by differential scanning calorimetry (DSC) and other thermal degradation studies [27,28], decrease of the work function due to the decomposition of PEDOT:PSS, as Diels–Alder reaction (SO_2 -extrusion), starts at higher temperatures (225–230 °C) from the ones used in this study (120 °C).

4. Summary and conclusions

The aging of PEDOT:PSS films 50 nm thick was investigated by dc conductivity measurements, X-ray and UV photoelectron spectroscopies for thermal treatment at 120 °C under environmental conditions. The electrical conductivity versus T followed the formula

$\sigma = \sigma_0 \exp[-(T_0/T)^\alpha]$, consistent with a carrier transport of the hopping type. The exponent α , decreased with aging from a value of ~ 1 for the fresh samples to a value ~ 0.5 at the end of the thermal treatment. This indicates a change in the conduction mechanism from the nearest-neighbour hopping at the beginning of the heat treatment to the charging-energy limited tunnelling between the conductive grains as thermal aging progresses. On the other hand the electrical conductivity at room temperature vs. t , the time of the heat treatment, decreased following the formula $\sigma = \sigma_1 \exp[-(t/\tau)^{1/2}]$, in agreement with a granular metal type structure, in which aging is due to the shrinking of the conductive grains, with $\tau = 96$ h. From the last formula the time t for which σ becomes half of its original value, is calculated to be 46.1 h in agreement with the value 46.3 h obtained from the $\sigma = \sigma(T)$ curves for different t . Moreover, the XPS and the UPS spectra before and after thermal degradation revealed a slight decrease of the insulating PSS from the surface. According to the proposed model thermal aging starts with an increase of the mobility of the hole polarons in PEDOT oligomers attached to insulating PSS chains, improving conductivity into the grains, which reduces α and increases σ_0 . At a second stage, the ionic bonds between PEDOT and PSS start to break, the PSS chains bearing negative charge at intervals align better themselves and PEDOT oligomers concentrate between them, further enhancing the conductivity of the grains. At the final stage the bonds between PEDOT and PSS break down, as XPS spectograms reveal. The conducting PEDOT being hydrophobic concentrates into the interior of the grains, although the insulating PSS being hydrophilic concentrates at the borders of the grains enhancing the potential barriers between the grains. These can explain the increase of σ_0 and T_0 with thermal treatment.

Acknowledgments

This work was partially financed by the Research Committee of the University of Patras under the framework of the “K. Karatheodori” program for basic research strengthening.

References

- [1] H. Burroughes, D.D.C. Bradley, A.R. Brown, R.N. Marks, K. Mackay, R.H. Friend, P.L. Burn, A.B. Holmes, Light-emitting diodes based on conjugated polymers, *Nature* 347 (6293) (1990) 539–541.
- [2] G. Yu, K. Pakbaz, A.J. Heeger, Semiconducting polymer diodes: large size, low cost photodetectors with excellent visible-ultraviolet sensitivity, *Applied Physics Letters* 64 (25) (1994) 3422–3424.
- [3] C.N. Hoth, S.A. Choulis, P. Schilinsky, C.J. Brabec, High photovoltaic performance of inkjet printed polymer:fullerene blends, *Advanced Materials* 19 (22) (2007) 3973–3978.
- [4] S.A. Choulis, A. Patwardhan, M.K. Mathai, V.-E. Choong, F. So, Interface modification to improve hole-injection properties in organic electronic devices, *Advanced Functional Materials* 16 (8) (2006) 1075–1080.
- [5] T.M. Brown, J.S. Kim, R.H. Friend, F. Cacialli, R. Daik, W.J. Feast, Built-in field electroabsorption spectroscopy of polymer light-emitting diodes incorporating a doped poly(3,4-ethylene dioxythiophene) hole injection layer, *Applied Physics Letters* 75 (12) (1999) 1679–1681.
- [6] J. Huang, P.F. Miller, J.S. Wilson, A.J. de Mello, J.C. de Mello, D.D.C. Bradley, Investigation of the effects of doping and post-deposition treatments on the conductivity, morphology and work function of poly(3,4-ethylenedioxythiophene)/poly(styrene sulfonate) films, *Advanced Functional Materials* 15 (2) (2005) 290–296.
- [7] I. Winter, C. Reese, J. Hormes, G. Heywang, F. Jonas, The thermal aging of poly(3,4-ethylenedioxythiophene). An investigation by X-ray absorption and X-ray photoelectron spectroscopy, *Chemical Physics* 194 (1) (1995) 207–213.
- [8] <<http://www.baytron.com/pages/985/scopeandlimitations.pdf>>.
- [9] H.H. Wieder, *Laboratory Notes of Electrical and Galvanomagnetic Measurements*, vol. 2, Elsevier, Amsterdam, 1979, ISBN 044441763X.
- [10] M.M. de Kok, M. Buechel, S.I.E. Vulto, P. van de Weijer, E.A. Meulenkaamp, S.H.P.M. de Winter, A.J.G. Mank, H.J.M. Vorstenbosch, C.H.L. Weijtens, V. van Elsbergen, Modification of PEDOT:PSS as hole injection layer in polymer LEDs, *Physica Status Solidi (a)* 201 (6) (2004) 1342–1359.
- [11] R.R. Smith, A.P. Smith, J.T. Stricker, B.E. Taylor, M.F. Durstock, Layer-by-layer assembly of poly(3,4-ethylenedioxythiophene):poly(styrenesulfonate), *Macromolecules* 39 (18) (2006) 6071–6074.
- [12] A.M. Nardes, M. Kemerink, R.A.J. Janssen, Anisotropic hopping conduction in spin-coated PEDOT:PSS thin films, *Physical Review B* 76 (8) (2007) 085208–085214.
- [13] A.M. Nardes, M. Kemerink, R.A.J. Janssen, J.A.M. Bastiaansen, N.M.M. Kiggen, B.M.W. Langeveld, A.J.J.M. van Breemen, M.M. de Kok, Microscopic understanding of the anisotropic conductivity of PEDOT:PSS thin films, *Advanced Materials* 19 (9) (2007) 1196–1200.
- [14] N. Mott, E.A. Davis, *Electronic Processes in Non-crystalline Materials*, Clarendon Press, Oxford, 1979, ISBN 0198512880.
- [15] E. Vitoratos, An analysis of DC conductivity in terms of degradation mechanisms induced by thermal aging in polypyrrole/polyaniline blends, *Current Applied Physics* 5 (6) (2005) 579–582.
- [16] E. Vitoratos, S. Sakkopoulos, E. Dalas, P. Malkaj, A. Anestis, D.C. conductivity and thermal aging of conducting zeolite/polyaniline and zeolite/polypyrrole blends, *Current Applied Physics* 7 (5) (2007) 578–581.
- [17] M.M. Fogler, S. Teber, B.I. Shklovskii, Variable-range hopping in quasi-one-dimensional electron crystals, *Physical Review B* 69 (3) (2004) 035413-1–035413-18.
- [18] M. Schreiber, H. Grussbach, Fluctuations in mesoscopic systems, *Philosophical Magazine B* 65 (4) (1992) 707–714.
- [19] M. Reghu, C.O. Yoon, C.Y. Yang, D. Moses, P. Smith, A.J. Heeger, Y. Cao, Transport in polyaniline networks near the percolation threshold, *Physical Review B* 50 (19) (1994) 13931–13941.
- [20] P. Sheng, J. Klafter, Hopping conductivity in granular disordered systems, *Physical Review B* 27 (4) (1983) 2583–2586.
- [21] L. Zuppiroli, M.N. Bussac, S. Paschen, Hopping in disordered conductivity polymers, *Physical Review B* 50 (8) (1994) 5196–5203.
- [22] A.N. Aleshin, S.R. Williams, A.J. Heeger, Transport properties of poly(3,4-ethylenedioxythiophene)/poly(styrenesulfonate), *Synthetic Metals* 94 (2) (1998) 173–177.
- [23] G. Greczynski, Th. Kugler, M. Keil, W. Osikowicz, M. Fahlman, W.R. Salanec, Photoelectron spectroscopy of thin films of PEDOT:PSS conjugated polymer blend: a mini-review and some new results, *Journal of Electron Spectroscopy and Related Phenomena* 121 (1–3) (2001) 1–17.
- [24] F. Petraki, S. Kennou, S. Nespurek, The electronic properties of the interface between nickel phthalocyanine and a PEDOT:PSS film, *Journal of Applied Physics* 103 (3) (2008) 033710-1–033710-15.
- [25] J. Hwang, F. Amy, A. Khan, Spectroscopic study on sputtered PEDOT. PSS: role of surface PSS layer, *Organic Electronics* 7 (5) (2006) 387–396.
- [26] K.Z. Xing, M. Fahlman, X.W. Chen, O. Inganas, W.R. Salanec, The electronic structure of poly(3,4-ethylene-dioxythiophene): studied by XPS and UPS, *Synthetic Metals* 89 (3) (1997) 161–165.
- [27] T.P. Nguyen, S.A. de Vos, An investigation into the effect of chemical and thermal treatments on the structural changes of poly(3,4-ethylenedioxythiophene)/polystyrenesulfonate and consequences on its use on indium tin oxide substrates, *Applied Surface Science* 221 (1–4) (2004) 330–339.
- [28] Y. Yosioka, G. Jabbar, Inkjet printing and patterning of PEDOT–PSS: application to optoelectronic devices, in: T.A. Skothein, J.R. Reynolds (Eds.), *Conjugated Polymers, Processing and Applications*, CRC Press, New York, 2007, pp. 3–1–3–21. ISBN 1420043609.